Results in Control and Optimization 17 (2024) 100484

Contents lists available at ScienceDirect

Results in Control and Optimization

journal homepage: www.elsevier.com/locate/rico

Attitude control of UAV bicopter using adaptive LQG

Fahmizal [a,b], Hanung Adi Nugroho [a,*], Adha Imam Cahyadi [a], Igi Ardiyanto [a]

[a] Department of Electrical and Information Engineering, Engineering Faculty, Universitas Gadjah Mada, Jl. Grafika No 2, Yogyakarta, 55281, Indonesia

[b] Department of Electrical Engineering and Informatics, Vocational College, Universitas Gadjah Mada, Jl. Yacaranda III, Yogyakarta, 55281, Indonesia

ARTICLE INFO

Keywords:
Attitude control
UAV bicopter
Adaptive LQG

ABSTRACT

This paper aims to design a controller that is able to maintain the stability of the unmanned aerial vehicle (UAV) bicopter attitude when carrying a payload. When the value of the payload inertia is in uncertainty, it is necessary to design a controller that can carry out the adaptation process. This paper proposes an Linear Quadratic Gaussian (LQG) adaptive controller to control the attitude of the bicopter with uncertain payload conditions. The proposed adaptive mechanism is a development of LQG control that can follow the response of the reference model. The success of LQG adaptive control is tested by providing uncertain payload parameters. The simulation results show that the LQG adaptive controller successfully overcomes the influence of inertial disturbances originating from the payload. There is a gain ρ in the LQG adaptive mechanism, this gain is influenced by the parameter σ which acts as a learning rate that produces a response to adapt to the response of the reference model. From the test results obtained when the value of σ is enlarged there is an increased overshoot condition/value but the root mean square error (RMSE) value decreases. That means when the RMSE decreases, the response is getting closer to the model reference. To reduce the overshoot effect of increasing the value of σ, an improvement is made in the search for the gain value of ρ. From the test results, the value of $\sigma = 1$ was chosen with the development of the gain equation ρ.

1. Introduction

Research on bicopter development on attitude control has played a crucial role. Bicopter requires a careful control strategy to maintain the stabilization and precision of its attitude motion. Several researchers have proposed linear control methods, such as Proportional–Integral–Derivative (PID) control [1–3] as an effective solution in maintaining the balance and attitude control of the bicopter.

Ozge et al. [1] researched the development of a bicopter flying robot. This robot is equipped with two rotary-wing units that are arranged in a tandem configuration on the chassis. A tilt mechanism is capable of tilting the rotors. Cascaded PID controllers are developed using dynamic models to regulate the robot's altitude and attitude. These control systems are simulated and subsequently implemented on a Naze32 flight controller that is connected to a Raspberry Pi for real-time operations. The system's real-time performance is both verified and evaluated, demonstrating its suitability for indoor robotic applications.

Zhang et al. [2] also investigated the construction of controllers that stabilize attitudes and the motion principle. They first created the model for the dynamics of twin-rotor aircraft. To find out its physical characteristics, they created and built a prototype.

* Corresponding author.
E-mail addresses: fahmizal@ugm.ac.id (Fahmizal), adinugroho@ugm.ac.id (H.A. Nugroho), adha.imam@ugm.ac.id (A.I. Cahyadi), igi@ugm.ac.id (I. Ardiyanto).

https://doi.org/10.1016/j.rico.2024.100484
Received 22 December 2023; Received in revised form 3 July 2024; Accepted 6 October 2024
Available online 11 October 2024

By assessing the final flight attitude tracking curve during an experiment, they confirmed that the bicopter's suggested PID attitude controller was accurate and effective.

The research conducted by Lukas et al. [3] describes the construction of a fully functional bicopter model at the laboratory scale and briefly discusses all associated control concerns. This work especially addresses the problem of stability when the aircraft is in flight and the design of the controllers and control loops using PID that correspond to it, which includes signal processing and measurement.

PID control in bicopter attitude is a common and effective method. PID control is based on the assumption that the system being controlled is linear and has fixed characteristics [4]. However, many real systems are non-linear, so PID controllers cannot produce optimal control in terms of performance and stability. In addition, PID control is more suitable for minimum-phase systems, which means that the system and the control are compatible [5]. However, when the phase of the system is opposite to the desired control, PID control can cause instability or poor response. PID control does not consider the uncertainty of the system parameters or the variability that may occur in the system during operation. When system parameters vary, PID control cannot produce optimal control. This is why PID control is less effective in dealing with systems with significant nonlinearity. Systems that have high nonlinearity require more complex and more specialized controller approaches.

Linear Quadratic Regulator (LQR) control is designed based on the optimal control principle, which optimizes a defined objective function (cost function) according to the desired control objective [6]. This can result in better performance in minimizing error, overshoot, or energy used in the system. In contrast, PID control assumes a precise model and cannot handle uncertainty well. In addition, LQR control allows free adjustment of the control parameters in the form of a state feedback gain matrix. This allows customization of the control characteristics according to the system's needs, providing greater flexibility than PID control.

LQR control is susceptible to uncertainties in the system model. If significant uncertainty or variability exists in the system parameters and dynamics, LQR control can result in poor performance or instability. On the other hand, the LQG controller is an extended LQR control with observations of the noise generated from the system to cope better with uncertainty [7]. In addition, LQR control does not consider the effect of noise on measurements or other noise in the system. This makes LQR control less effective in dealing with disturbances or noise that can significantly affect system performance.

When a system has significant uncertainty, noise, or non-linearity, LQG control has the advantage of combining optimal control of LQR with optimal estimation of state and noise, which results in better control performance and adaptability to varying system conditions. However, LQG control also requires accurate measurements and precise models and can be more complex to implement [8].

Inertial disturbances in the form of payload on a bicopter can significantly affect its attitude control. Inertia is a physical property of a body that affects its response to rotational motion. In a bicopter, inertia includes the mass, moment of inertia, and mass distribution of the two main rotors and other parts of the mechanical structure of the bicopter. Inertial disturbances can cause the rotational response to slow down or overshoot and be disproportionate to the desired control change. This can delay achieving stabilization or proper adjustments in the roll, pitch, or yaw angles of the bicopter. In addition, unbalanced structure and mass distribution or inappropriate inertia can cause overshooting (exceeding the desired value) or underdamping (prolonged vibration) phenomena when the bicopter undergoes attitude changes. This can compromise the stability and performance of the control system.

High inertial disturbances can cause the bicopter to experience delays in responding to changes in angular velocity (rotation). This lack of responsiveness can hinder the bicopter's ability to maneuver quickly and precisely. Therefore, accounting for the effects of inertial disturbances is essential in designing and implementing attitude control systems for bicopter. Using an adaptive control approach, control optimization can help overcome the challenges caused by inertial disturbances and improve the control performance of the bicopter attitude.

Research conducted by Qin et al. [9] describes a bicopter design named Gemini. This research discusses the process of making the Gemini platform from selecting the ideal propeller through aerodynamic analysis, system design, optimization, and control implementation. In its application, Gemini attitude control uses PID control in a cascaded manner Furthermore, in the research of Qin et al. [10] proposed a servoless concept, but this concept requires a magnetic encoder sensor in the cyclic blade system and of course this concept requires high costs in its design. This research also has not added inertial disturbance analysis to the system model.

Research conducted by Xiang et al. [11] proposed moving the center of mass (CoM) of the bicopter to the top. In this study, using PID control on bicopter attitude with tuning using particle swarm optimization (PSO) but has not added inertial disturbance analysis to the system model. Furthermore, research conducted by Hu et al. [12] proposed the addition of an inverted pendulum to maintain attitude stability during hovering using PID control. This research has not added inertial disturbance analysis to the system model.

From the literature review, it is common to use PID controllers on bicopter attitude and has not added inertial disturbance analysis in the form of payload. The presence of inertial disturbances in a bicopter can significantly affect its attitude control. Inertial disturbances can cause the rotational response to be slower or experience overshoot and disproportionate to the desired control change. Further research is needed to identify and design adaptive and optimal controls that can cope with variations in the dynamics of the bicopter.

The development of LQG adaptive control method aims to combine the advantages of optimal control of LQG with adaptive ability to overcome the uncertainty and variation of dynamics in bicopter. The contribution of this paper is in the form of designing an adaptation mechanism into the LQG control structure for bicopter attitude control. Furthermore, to evaluate the performance and stability of the LQG adaptive control system for bicopter attitude is essential. The simplest concepts of stability, namely Lyapunov stability [13], BIBO stability [14], and Ulam–Hyers stability [15,16]. Comparison of the performance of LQG adaptive control with LQR control can help demonstrate the superiority of LQG adaptive controller under changing dynamic conditions.

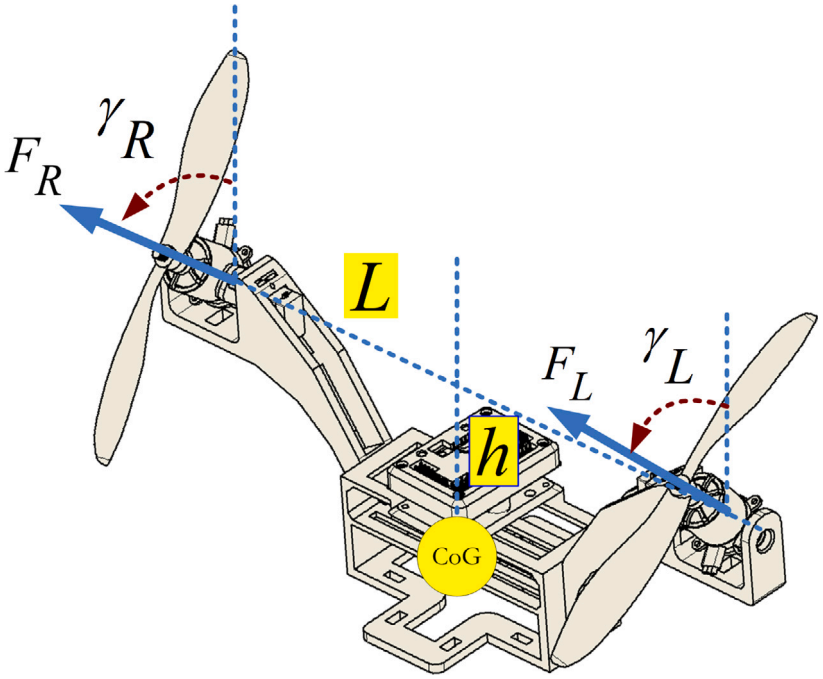

Fig. 1. Body diagram of bicopter.

2. Methodology

2.1. Dynamics modeling of a bicopter

This sub-chapter discusses the modeling of the bicopter system observed in a Cartesian diagram frame with three-dimensional axes (x, y, z). The frame diagram is divided into two, namely the earth frame which is not moving, and the bicopter body frame (body frame). The linear position of the bicopter (Γ^E) is determined from the vector coordinates between the origin of the body frame (B-frame) and the origin of the earth frame (E-frame) with respect to the Eframe. The angular position of the bicopter (Θ^E) is determined from the orientation of the B-frame to the E-frame. The linear position and angular position are defined respectively as,

$$\Gamma^E = \begin{bmatrix} x & y & z \end{bmatrix}, \tag{1}$$

$$\Theta^E = \begin{bmatrix} \phi & \theta & \psi \end{bmatrix}. \tag{2}$$

Next, the bicopter rotates about the (x, y, z) axis using the rotation matrix. Bicopter speed consists of linear velocity $\begin{bmatrix} \dot{x} & \dot{y} & \dot{z} \end{bmatrix}$ and angular velocity $\begin{bmatrix} \dot{\phi} & \dot{\theta} & \dot{\psi} \end{bmatrix}$ so that when represented in state space form, the bicopter equation has twelve states which are divided into two categories, six states translation and six rotational states as,

$$x_{1-6} = \begin{bmatrix} x & \dot{x} & y & \dot{y} & z & \dot{z} \end{bmatrix}^T, \tag{3}$$

$$x_{7-12} = \begin{bmatrix} \phi & \dot{\phi} & \theta & \dot{\theta} & \psi & \dot{\psi} \end{bmatrix}^T. \tag{4}$$

Right rotor thrust (F_R) and left rotor thrust (F_L) generated by the propeller and rotor and their components in the x and z directions are shown in Fig. 1. In addition, the right side tilt angle and left are denoted as γ_R and γ_L. Using Newton's second law, the equations of forces in the x, y and z directions are defined as,

$$\sum F_x = F_R \sin\gamma_R + F_L \sin\gamma_L, \tag{5}$$

$$\sum F_y = 0, \tag{6}$$

$$\sum F_z = F_R \cos\gamma_R + F_L \cos\gamma_L. \tag{7}$$

From the input u as follows,

$$u = \begin{bmatrix} u_1 & u_2 & u_3 & u_4 \end{bmatrix}^T, \tag{8}$$

$$u_1 = C_T \left(\Omega_R^2 \cos\gamma_R + \Omega_L^2 \cos\gamma_L \right), \tag{9}$$

$$u_2 = C_T \left(\Omega_R^2 \cos\gamma_R - \Omega_L^2 \cos\gamma_L \right), \tag{10}$$

$$u_3 = C_T \left(\Omega_R^2 \sin\gamma_R + \Omega_L^2 \sin\gamma_L \right), \tag{11}$$

$$u_4 = C_T \left(\Omega_R^2 \sin\gamma_R - \Omega_L^2 \sin\gamma_L \right). \tag{12}$$

We can calculate the bicopter's total lift (thrust) and moment of force. Where C_T is the propeller's thrust coefficient. Ω_R and Ω_L represent the rotors' right and left rotational speeds, and γ_R and γ_L represent the rotors' right and left tilt angles.

The rotation subsystem (roll, pitch, and yaw) is the inner loop, and the translation subsystem (x, y position, and z (altitude)) is the outer loop. Based on the dynamic solution of the model using Newton–Euler [1,2,17]. The translational motion are defined as,

$$\ddot{x} = -\frac{1}{m} \left(s\phi s\psi + c\phi s\theta c\psi \right) u_1 - \frac{c\theta c\psi}{m} u_3, \tag{13}$$

$$\ddot{y} = -\frac{1}{m} \left(-s\phi c\psi + c\phi s\theta s\psi \right) u_1 + \frac{c\theta s\psi}{m} u_3, \tag{14}$$

$$\ddot{z} = g - \frac{1}{m} \left(c\phi c\theta \right) u_1 - \frac{s\theta}{m} u_3. \tag{15}$$

And the rotational motion are defined as,

$$\ddot{\phi} = \frac{L}{I_{xx}} u_2, \tag{16}$$

$$\ddot{\theta} = \frac{h}{I_{yy}} u_3, \tag{17}$$

$$\ddot{\psi} = \frac{L}{I_{zz}} u_4, \tag{18}$$

where $s = sin$ and $c = cos$.

2.2. Inertial disturbance modeling

By attaching a payload to the bicopter, it is possible to model inertial disturbances. Previously, it was presumed that the bicopter operated under nominal conditions (J_0), so the inertial matrix was diagonal according to

$$J_0 = \begin{bmatrix} I_{xx} & 0 & 0 \\ 0 & I_{yy} & 0 \\ 0 & 0 & I_{zz} \end{bmatrix}. \tag{19}$$

However, when provided payload, the bicopter's inertial matrix will undoubtedly change. In order to facilitate the analysis, the inertial matrix is separated into two types: the inertial matrix at nominal conditions and the inertial matrix that results from the presence of payload (ΔJ) as follows,

$$\Delta J = \begin{bmatrix} \Delta I_{xx} & 0 & 0 \\ 0 & \Delta I_{yy} & 0 \\ 0 & 0 & \Delta I_{zz} \end{bmatrix}. \tag{20}$$

The value of ΔJ is affected by the products' mass, shape, and position of payload. The addition of the inertial matrix that appears due to the presence of payload referred to as the perturbed inertia matrix (J_δ), allowing the inertial matrix to be written as,

$$J_\delta = J_0 + \Delta J. \tag{21}$$

It is assumed that the bicopter's payload will carry a solid cubic-shaped block filled with liquid as shown in Fig. 2 with the specifications in Table 1. Because the payload is in the form of blocks, the inertial disturbance matrix is a symmetric matrix with zero off-diagonal elements as in Eq. (20), with the matrix elements consisting as follows,

$$\Delta I_{xx} = \frac{m}{12} \left(d^2 + h^2 \right), \tag{22}$$

$$\Delta I_{yy} = \frac{m}{12} \left(d^2 + w^2 \right), \tag{23}$$

$$\Delta I_{zz} = \frac{m}{12} \left(h^2 + w^2 \right). \tag{24}$$

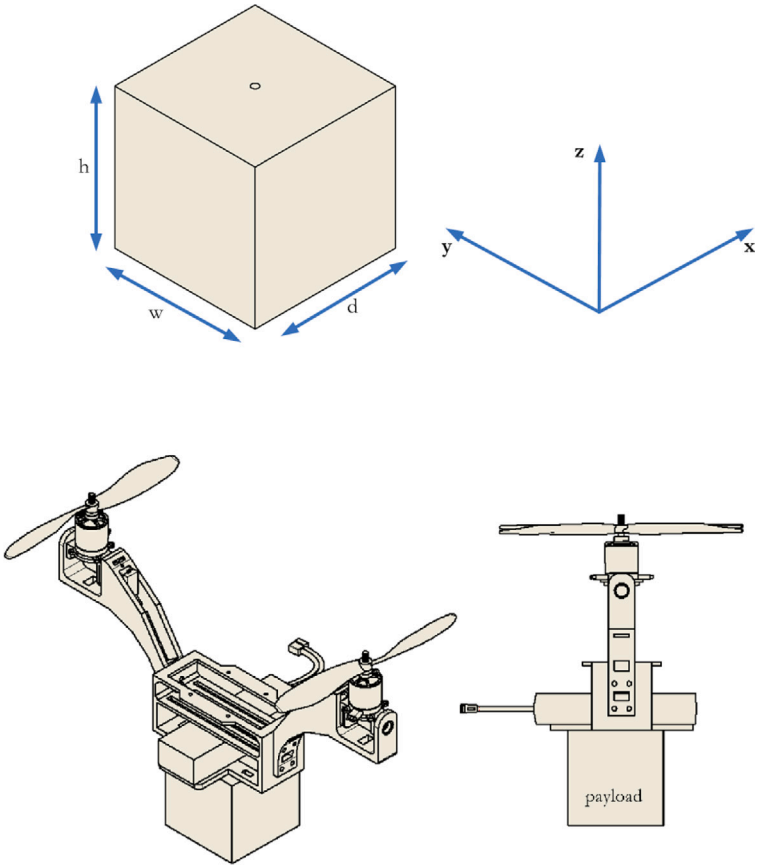

Fig. 2. Models of payloads.

Table 1
Payload specifications.

Parameter	Value	Units
Mass	0.2	kg
Length (d)	0.08	m
Width (w)	0.08	m
Height (h)	0.08	m

2.3. Attitude bicopter modeling

2.3.1. No inertial disturbance

From the dynamics model in Eq. (16) – Eq. (18), it is known that the bicopter attitude system has a decoupling condition so that the dynamics equation of the attitude roll movement can be obtained as follows,

$$\frac{\Phi}{U_{2(s)}} = \frac{\alpha}{s^2}, \tag{25}$$

$$\frac{\Theta}{U_{3(s)}} = \frac{\beta}{s^2}, \tag{26}$$

$$\frac{\Psi}{U_{4(s)}} = \frac{\gamma}{s^2}, \tag{27}$$

where $\alpha = \frac{L}{I_{xx}}$, $\alpha = \frac{h}{I_{yy}}$ and $\alpha = \frac{L}{I_{zz}}$.

In Eq. (25), it can be written into state space form as follows,

$$\begin{aligned} \dot{x} &= A_\phi x + B_\phi u_2 \\ A_\phi &= \begin{bmatrix} 0 & 1 \\ 0 & 0 \end{bmatrix} \begin{bmatrix} x_1 \\ x_2 \end{bmatrix}, B_\phi = \begin{bmatrix} 0 \\ \alpha \end{bmatrix} u_2. \end{aligned} \tag{28}$$

If the closed-loop characteristic equation of attitude roll is known in Eq. (28), it can be obtained using $det\left(sI-\left(A_\phi-B_\phi K_\phi\right)\right)=0$, with the following explanation,

$$\begin{aligned}
&det\left(sI-(A_\phi-B_\phi K_\phi)\right)=0\\
&\left|s\begin{bmatrix}1&0\\0&1\end{bmatrix}-\left(\begin{bmatrix}0&1\\0&0\end{bmatrix}-\begin{bmatrix}0\\\alpha\end{bmatrix}\begin{bmatrix}K_{1\phi}&K_{2\phi}\end{bmatrix}\right)\right|=0\\
&\left|\begin{bmatrix}s&0\\0&s\end{bmatrix}-\begin{bmatrix}0&1\\0&0\end{bmatrix}-\begin{bmatrix}0&0\\\alpha K_{1\phi}&\alpha K_{2\phi}\end{bmatrix}\right|=0\\
&\left|\begin{bmatrix}s&0\\0&s\end{bmatrix}-\begin{bmatrix}0&1\\-\alpha K_{1\phi}&-\alpha K_{2\phi}\end{bmatrix}\right|=0\\
&\left|\begin{bmatrix}s&-1\\\alpha K_{1\phi}&s+\alpha K_{2\phi}\end{bmatrix}\right|=0\\
&s^2+\left(\alpha K_{2\phi}\right)s+\alpha K_{1\phi}=0
\end{aligned}\tag{29}$$

It is known that the characteristic equation of a closed second-order system in general can be defined as,

$$s^2+2\zeta\omega_n s+\omega_n^2=0,\tag{30}$$

where ζ is the damping ratio and ω_n is the natural frequency. By using the substitution method, the gains $K_{1\phi}$ and $K_{2\phi}$ can be determined according to ζ and ω_n based on the desired system performance are defined as follows,

$$K_{1\phi}=\frac{\omega_n^2}{\alpha}=\frac{I_{xx}\omega_n^2}{L},\tag{31}$$

$$K_{2\phi}=\frac{2\zeta\omega_n}{\alpha}=\frac{I_{xx}2\zeta\omega_n}{L}.\tag{32}$$

With the same steps, the state feedback gain on the pitch attitude dynamics can be obtained as follows,

$$K_{1\theta}=\frac{\omega_n^2}{\beta}=\frac{I_{yy}\omega_n^2}{h},\tag{33}$$

$$K_{2\theta}=\frac{2\zeta\omega_n}{\beta}=\frac{I_{yy}2\zeta\omega_n}{h}.\tag{34}$$

And the state feedback gain on the dynamics of the yaw attitude movement are defined as follows,

$$K_{1\psi}=\frac{\omega_n^2}{\gamma}=\frac{I_{zz}\omega_n^2}{L},\tag{35}$$

$$K_{2\psi}=\frac{2\zeta\omega_n}{\gamma}=\frac{I_{zz}2\zeta\omega_n}{L}.\tag{36}$$

2.3.2. With inertial disturbance

Suppose there is a defined inertial disturbance in the form of a payload. In that case, the dynamics of the roll attitude movement can be written as,

$$\breve{\Phi}=\frac{1}{s^2}\left(\frac{L}{I_{xx}+\Delta I_{xx}}\right)U_{2(s)}.\tag{37}$$

The dynamics of the pitch movement can be written as,

$$\breve{\Theta}=\frac{1}{s^2}\left(\frac{h}{I_{yy}+\Delta I_{yy}}\right)U_{3(s)},\tag{38}$$

and the dynamics of the yaw attitude movement can be written as,

$$\breve{\Psi}=\frac{1}{s^2}\left(\frac{L}{I_{zz}+\Delta I_{zz}}\right)U_{4(s)}.\tag{39}$$

In Eq. (37), it can be written into state space form as follows,

$$\begin{aligned}
&\dot{x}=\breve{A}_\phi x+\breve{B}_\phi u_2,\\
&\breve{A}_\phi=\begin{bmatrix}0&1\\0&0\end{bmatrix}\begin{bmatrix}x_1\\x_2\end{bmatrix},\breve{B}_\phi=\begin{bmatrix}0\\\frac{L}{I_{xx}+\Delta I_{xx}}\end{bmatrix}u_2.
\end{aligned}\tag{40}$$

If the closed-loop characteristic equation of attitude roll is known in Eq. (40), it can be obtained using $det\left(sI-\left(\breve{A}_\phi-\breve{B}_\phi K_\phi\right)\right)=0$,

with the following explanation,

$$\begin{aligned}
&det\left(sI-(\breve{A}_{\phi}-\breve{B}_{\phi}K_{\phi})\right)=0\\
&\left|s\begin{bmatrix}1&0\\0&1\end{bmatrix}-\left(\begin{bmatrix}0&1\\0&0\end{bmatrix}-\begin{bmatrix}0\\\frac{L}{I_{xx}+\Delta I_{xx}}\end{bmatrix}\begin{bmatrix}K_{1\phi}&K_{2\phi}\end{bmatrix}\right)\right|=0\\
&\left|\begin{bmatrix}s&0\\0&s\end{bmatrix}-\begin{bmatrix}0&1\\0&0\end{bmatrix}-\begin{bmatrix}0&0\\\left(\frac{L}{I_{xx}+\Delta I_{xx}}\right)K_{1\phi}&\left(\frac{L}{I_{xx}+\Delta I_{xx}}\right)K_{2\phi}\end{bmatrix}\right|=0\\
&\left|\begin{bmatrix}s&0\\0&s\end{bmatrix}-\begin{bmatrix}0&1\\-\left(\frac{L}{I_{xx}+\Delta I_{xx}}\right)K_{1\phi}&-\left(\frac{L}{I_{xx}+\Delta I_{xx}}\right)K_{2\phi}\end{bmatrix}\right|=0\\
&\left|\begin{bmatrix}s&-1\\\left(\frac{L}{I_{xx}+\Delta I_{xx}}\right)K_{1\phi}&s+\left(\frac{L}{I_{xx}+\Delta I_{xx}}\right)K_{2\phi}\end{bmatrix}\right|=0\\
&s^2+\left(\left(\frac{L}{I_{xx}+\Delta I_{xx}}\right)K_{2\phi}\right)s+\left(\frac{L}{I_{xx}+\Delta I_{xx}}\right)K_{1\phi}=0
\end{aligned}\tag{41}$$

then the state feedback gain can be determined according to ζ and ω_n based on the desired system performance with $K_{1\phi}$ as,

$$K_{1\phi}=\frac{\omega_n^2}{\left(\frac{L}{I_{xx}+\Delta I_{xx}}\right)}\tag{42}$$

and $K_{2\phi}$ as,

$$K_{2\phi}=\frac{2\zeta\omega_n}{\left(\frac{L}{I_{xx}+\Delta I_{xx}}\right)}\tag{43}$$

for attitude roll dynamics.

The state feedback gain on the dynamics of attitude pitch movement are defined as follows,

$$K_{1\theta}=\frac{\omega_n^2}{\left(\frac{h}{I_{yy}+\Delta I_{yy}}\right)},\tag{44}$$

$$K_{2\theta}=\frac{2\zeta\omega_n}{\left(\frac{h}{I_{yy}+\Delta I_{yy}}\right)}.\tag{45}$$

And the state feedback gain on the dynamics of the yaw attitude movement are defined as follows,

$$K_{1\psi}=\frac{\omega_n^2}{\left(\frac{L}{I_{zz}+\Delta I_{zz}}\right)},\tag{46}$$

$$K_{2\psi}=\frac{2\zeta\omega_n}{\left(\frac{L}{I_{zz}+\Delta I_{zz}}\right)}.\tag{47}$$

2.4. Model reference adaptive control (MRAC)

The original way to use MRAC was through the Massachusetts Institute of Technology (MIT) rule. It was made at MIT's Instrumentation Laboratory, which is now called the Draper Laboratory, which is where the name comes from [18].

To present the MIT rule, we will consider a closed-loop system in which the controller has one adjustable parameter θ. The desired closed-loop response is specified by a model whose output is y_m. Let e be the error between the output y of the closed-loop system and the output y_m of the model. One possibility is to adjust parameters in such a way that the loss function

$$J(\theta)=\frac{1}{2}e^2\tag{48}$$

is minimized. To make J small, it is reasonable to change the parameters in the direction to the negative gradient of J, that is,

$$\frac{d\theta}{dt}=-\gamma\frac{\partial J}{\partial\theta}=-\gamma e\frac{\partial e}{\partial\theta}\tag{49}$$

This the celebrate *MIT rule*. The partial derivative $\frac{\partial e}{\partial\theta}$, which is called the *sensitivity derivative* of the system. Tells how the error is influenced by the adjustable parameter. If it is assumed that the parameter changes are slower than the other variables in the system, then the derivative $\frac{\partial e}{\partial\theta}$ can be evaluated under the assumption that θ is constant.

There are many alternatives to loss function give by Eq. (48). If it is chosen to be

$$J(\theta)=|e|\tag{50}$$

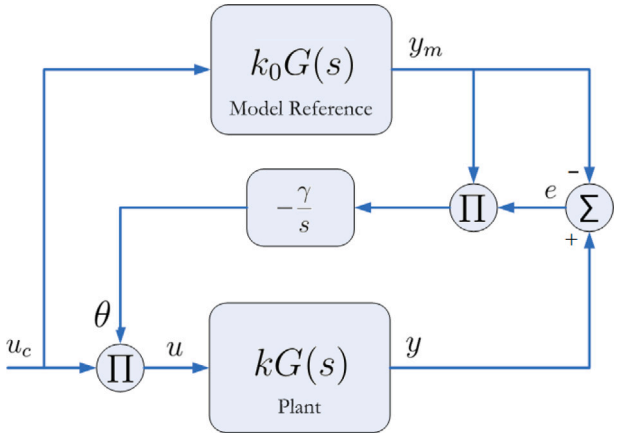

Fig. 3. Direct MRAC control block design with a plant model of order one using MIT rules.

the gradient method gives

$$\frac{d\theta}{dt} = -\gamma \frac{\partial e}{\partial \theta} \text{ sign } e \tag{51}$$

Consider the problem of adjusting a feedforward gain as shown in Fig. 3. In this problem it is assumed that the process is linear with the transfer function $kG(s)$, where $G(s)$ is known and k is an unknown parameter. The underlying design problem is to find a feedforward controller that gives a system with the transfer function $G_m(s) = k_0G(s)$, where k_0 is a given constant. With the feedforward controller

$$u = \theta u_c \tag{52}$$

where u is the control signal and u_c the command signal, the transfer function from command signal to the output becomes $\theta kG(s)$. This transfer function is equal to $G_m(s)$ if the parameter θ is chosen to be

$$\theta = \frac{k_0}{k}. \tag{53}$$

We will now use the MIT rule to obtain a method for adjusting the parameter θ when k is not known. The error is

$$e = y - y_m = kG(p)\theta u_c - k_0G(p)u_c \tag{54}$$

where u_c is the command signal, y_m is the model output, y is the process output, θ is the adjustable parameter, and $p = \frac{d}{dt}$ is the differential operator. The sensitivity derivative is given by

$$\frac{\partial e}{\partial \theta} = kG(p)u_c = \frac{k}{k_0} y_m. \tag{55}$$

The MIT rule then gives the following adaptation law:

$$\frac{d\theta}{dt} = -\gamma' \frac{k}{k_0} y_m e = -\gamma y_m e, \tag{56}$$

where $\gamma = \gamma' \frac{k}{k_0}$ has been introduced instead of γ'. Notice that to have the correct sign of γ, it is necessary to know the sign of k. Eq. (56) gives law for adjusting the parameter.

3. Adaptive LQG control design

By referring to the MRAC method using MIT rules, the LQG adaptive controller design for the bicopter attitude roll is presented in Fig. 4 and Algorithm 1, which can be applied with the following explanation:

1. Model reference, this section is a reference model which aims to ensure that the results of the controller have closed loop system behavior in accordance with the desired reference model. In other words, how can the system as a whole behave in accordance with the reference model. In this subchapter, it is designed so that the attitude roll controller has response characteristics such as those in the dynamic model as follows,

$$Y_m = \frac{1950}{s^2 + 331s + 1950}. \tag{57}$$

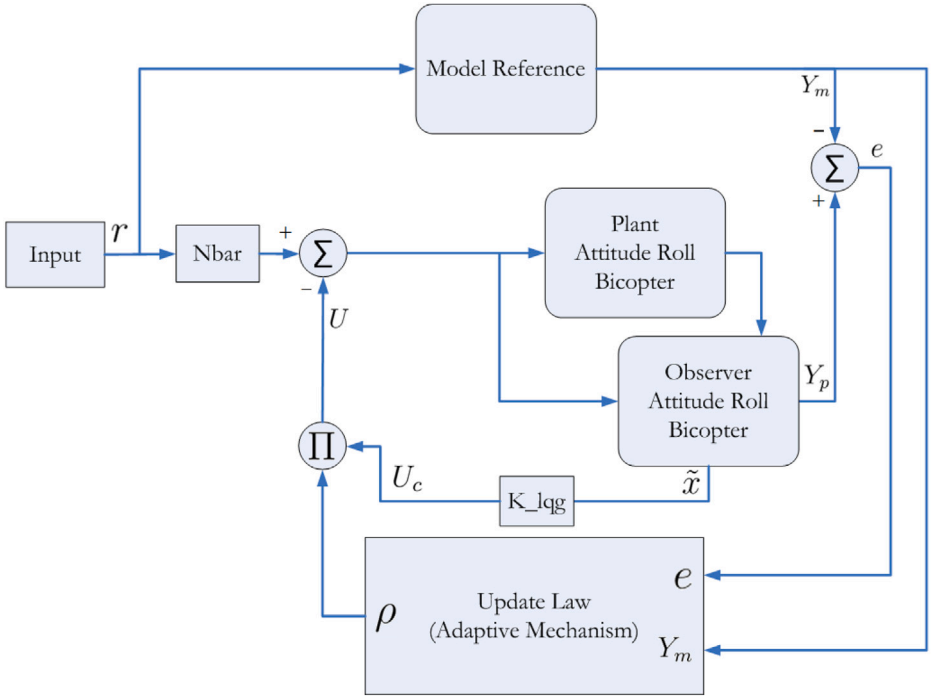

Fig. 4. LQG adaptive control block design for attitude roll bicopter.

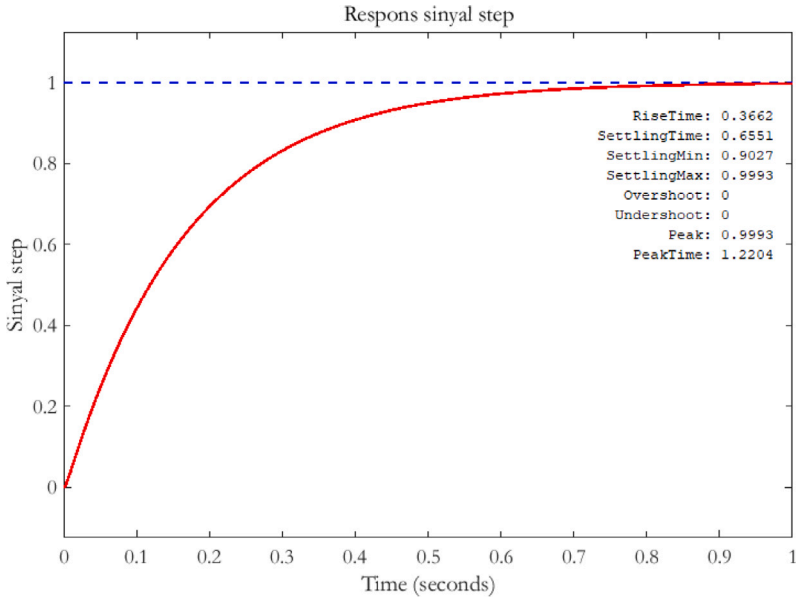

Fig. 5. Step signal response in reference model.

The open loop step response model Eq. (57) as presented in Fig. 5, the system characteristic parameters can be seen as follows: rise time (0.3662 s), settling time (0.6551 s) and steady state error (0) which desired. The model reference output (Y_m) is the reference path that the plant output (Y_p) must follow.

2. Model plant, this part is the attitude roll dynamics equation where there is inertial interference from the payload. The value of the payload inertia can vary and is unknown, therefore the plant output value (Y_p) will always change when using fixed control parameters. Changes in controlling parameters must also accompany changes in plant dynamics. When output (Y_p) is expected to be able to follow the reference model of (Y_m)), then it can be obtained $error(e) = Y_p - Y_m$.

3. Adaptive controller, this section consists of two control sub-components, namely:

   - *Adaptive mechanism*, the purpose of this section is to produce output in the form of gain rho (ρ) which is the integral of rho dot as

   $$\dot{\rho} = \sigma Y_m e. \tag{58}$$

   $\dot{\rho}$ is obtained based on the error (e) by multiplying the output of the reference model (Y_m) and multiplying by sigma (σ). How fast the adaptation process is depends on the parameter σ which is called the learning rate. The greater the value of σ, the faster the plant adapts to dynamic changes. Eq. (58) can be developed to ensure that e gets closer to zero. In this paper, we develop the gain rho (ρ) equation into

   $$\dot{\rho} = \left(\alpha \dot{e} + \beta \int e(t)dt\right) \sigma Y_m e, \tag{59}$$

   with additional gain in the form of parameters α and β.
   - LQG *controller*, the control signal resulting from the gain state feedback using LQG is denoted by U_c and then multiplied by the gain ρ, the control signal U can be obtained as,

   $$U = \rho\, U_c. \tag{60}$$

Algorithm 1 LQG Adaptive Control.

Initialization:
    Initialize linear system matrices: A, B, C, D
    Initialize cost matrices: Q, R, matrices covariance: w, v
    Initialize initial state vector: $x(0)$, control input: $u(0)$
    Initialize model reference, get pole (p_1, p_2) from model reference
    Initialize σ

Design Kalman filter gain matrix L:
    Compute $L = lqe(A, w, C, w, v)$

LQG Controller Design:
if use pole placement **then**
        Compute $K = place((A - LC), B, [-p_1 - p_2])$
else if use LQR **then**
        Compute $K = lqr((A - LC), B, Q, R)$
end if

Control Loop:
while each time step k **do**
    Measure the output $y(k)$
    Estimate the state $\tilde{x}(k)$ using Kalman filter:
        $\tilde{x}(k) = A\tilde{x}(k-1) + Bu(k-1) + L(y(k) - C\tilde{x}(k-1))$
    Compute the control input:
        $U_c(k) = -K\tilde{x}(k)$

Adaptive Mechanism:
    Get Y_m and calculate error:
        $e = Y_p - Y_m$ ▷ $Y_p = y(k)$
    Calculate gain ρ:
        $\dot{\rho} = \left(\alpha \dot{e} + \beta \int e(t)dt\right) \sigma Y_m e$
    Apply control input U to the system
        $U = \rho\, U_c$
end while

4. Simulation results and discussion

This section discusses the testing of the controller applied to control the attitude roll stability of the bicopter. There are three test scenarios, first when the nominal condition (not yet given inertial disturbance), second by giving a predetermined payload inertia value, and the third with an unknown value of payload inertia. Table 2 shows the bicopter parameters for simulations.

Table 2
Bicopter dynamic model parameters.

Parameter	Symbols	Value	Unit
Mass of the bicopter	m	0.725	kg
Gravitational acceleration	g	9.81	m s^{-2}
Vertical distance between CoG and center of the rotor	h	0.042	m
Horizontal distance CoG and rotor center	L	0.225	m
Thrust coefficient	C_T	0.1222	–
The moment of inertia along x axis	I_{xx}	0.116×10^{-3}	kg m^2
The moment of inertia along y axis	I_{yy}	0.0408×10^{-3}	kg m^2
The moment of inertia along z axis	I_{zz}	0.105×10^{-3}	kg m^2

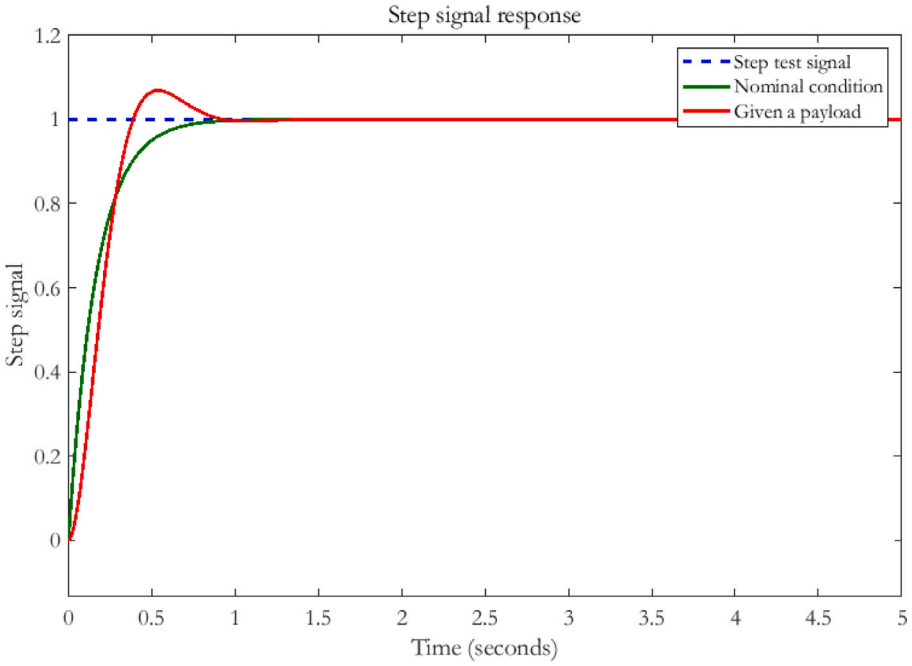

Fig. 6. Step test signal response in attitude roll dynamics using gain state feedback $K_{1\phi} = 1.0053$ and $K_{2\phi} = 0.1706$.

4.1. Scenario 1

If the nominal value of attitude roll inertia is known ($I_{xx} = 0.116 \times 10^{-3}$ kg m^2), by planning that the system has the appropriate characteristics at $s^2 + 331s + 1950 = 0$, then it is known that $2\zeta\omega_n = 331$, $\omega_n^2 = 1950$ and the system pole is at $s_1 = -6$ and $s_2 = -325$ so that the gain

$$K_{1\phi} = \frac{\omega_n^2}{\alpha} = \frac{I_{xx}\omega_n^2}{L} = 1.0053, \tag{61}$$

and

$$K_{2\phi} = \frac{2\zeta\omega_n}{\alpha} = \frac{I_{xx}2\zeta\omega_n}{L} = 0.1706 \tag{62}$$

is obtained using the pole placement technique as described in Eqs. (31) and (32) with response results as in Fig. 6 and Table 3.

The line red response in Fig. 6 is the condition when the attitude roll system is coupled with payload inertia, it can be seen that the response experiences overshoot when using the gain parameters $K_{1\phi} = 1.0053$ and $K_{2\phi} = 0.1706$. To eliminate this overshoot of course it is necessary to change the value of the gain state feedback because the attitude roll dynamics have changed due to the inertia of the payload. In the second scenario test, a gain state feedback parameter was obtained, which was able to eliminate overshoot when the payload inertia was increased.

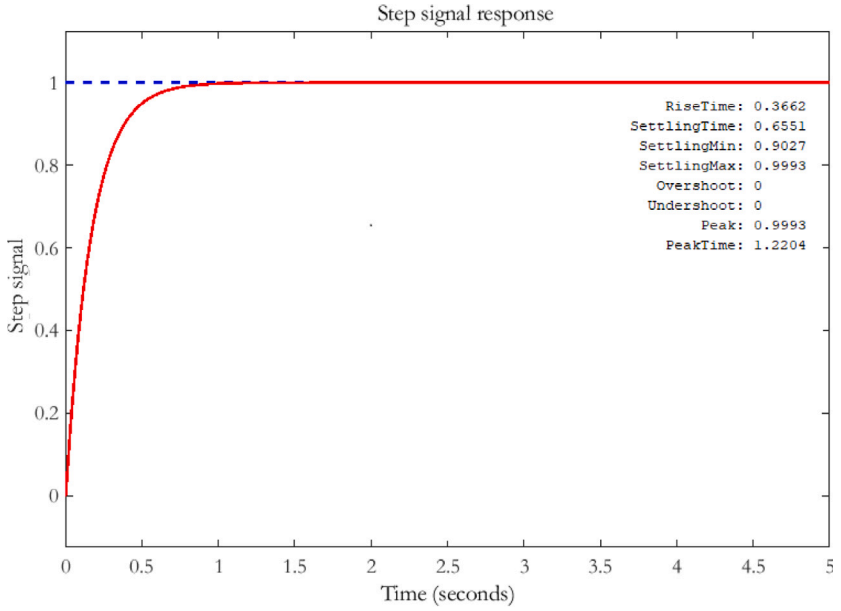

Fig. 7. Step test signal response in attitude roll dynamics using gain state feedback $K_{1\phi} = 33.5053$ and $K_{2\phi} = 5.6873$.

Table 3
Characteristics response after being given a step test signal with gain state feedback $K_{1\phi} = 1.0053$ and $K_{2\phi} = 0.1706$.

Characteristics	Attitude roll inertia condition	
	Nominal condition	After being given the payload
Rise Time (s)	0.3662	0.2589
Settling Time (s)	0.6551	0.7853
Settling Min	0.9027	0.9005
Settling Max	0.9993	1.0685
Overshoot (%)	0	6.8458

4.2. Scenario 2

If the initial nominal value of inertia is known ($I_{xx} = 0.116 \times 10^{-3}$ kg m^2) and payload inertia ($\Delta I_{xx} = 0.0037$ kg m^2). By planning that the system has the appropriate characteristics at $s^2 + 331s + 1950 = 0$, it is known that $2\zeta\omega_n = 331$, $\omega_n^2 = 1950$ and the system poles are at $s_1 = -6$ and $s_2 = -325$ so that the gain

$$K_{1\phi} = \frac{\omega_n^2}{\left(\frac{L}{I_{xx}+\Delta I_{xx}}\right)} = \frac{1950}{\left(\frac{0.225}{0.116\times10^{-3}+0.0037}\right)} = 33.5053, \tag{63}$$

and

$$K_{2\phi} = \frac{2\zeta\omega_n}{\left(\frac{L}{I_{xx}+\Delta I_{xx}}\right)} = \frac{331}{\left(\frac{0.225}{0.116\times10^{-3}+0.0037}\right)} = 5.6873 \tag{64}$$

can be obtained using the pole placement technique as described Eqs. (42) and (43). The test results of the closed loop control step response $K_{1\phi} = 33.5053$ and $K_{2\phi} = 5.6873$ are presented in Fig. 7.

From Fig. 7, it can be seen that the response results with the step test signal produce a fast settling time value of 0.6551 s and the system does not experience overshoot. Furthermore, if a comparison is carried out using the LQR technique, the gain state feedback $K_{1\phi}$ and $K_{2\phi}$ is obtained with results in accordance with the Q matrix and R matrix tuning processes. In testing using LQR control, variations in the Q matrix values are carried out as in Table 4 with the R matrix value set at 0.1. The results of step signal testing using LQR control with Q matrix variations are presented in Fig. 8.

The response comparison of the gain state feedback using the pole placement technique with the LQR technique is presented in Fig. 9. Table 5 shows the results of the comparison of the response characteristics. Observing these response characteristics indicates that the LQR technique produces a more optimal response when appropriate in the selection of matrix Q and matrix R.

Table 4
Variation of Q matrix weighting values.

No	Q weighting matrix	Gain state feedback K with LQR
1	$Q = \begin{bmatrix} 10 & 0 \\ 0 & 0.1 \end{bmatrix}$	$K_{1\phi} = 10.0000,\ K_{2\phi} = 1.0051$
2	$Q = \begin{bmatrix} 1 & 0 \\ 0 & 0.1 \end{bmatrix}$	$K_{1\phi} = 3.1623,\ K_{2\phi} = 1.0016$
No	Matriks pembobot Q	*Gain state feedback* K dengan LQR
3	$Q = \begin{bmatrix} 0.1 & 0 \\ 0 & 0.1 \end{bmatrix}$	$K_{1\phi} = 1.0000,\ K_{2\phi} = 1.0005$

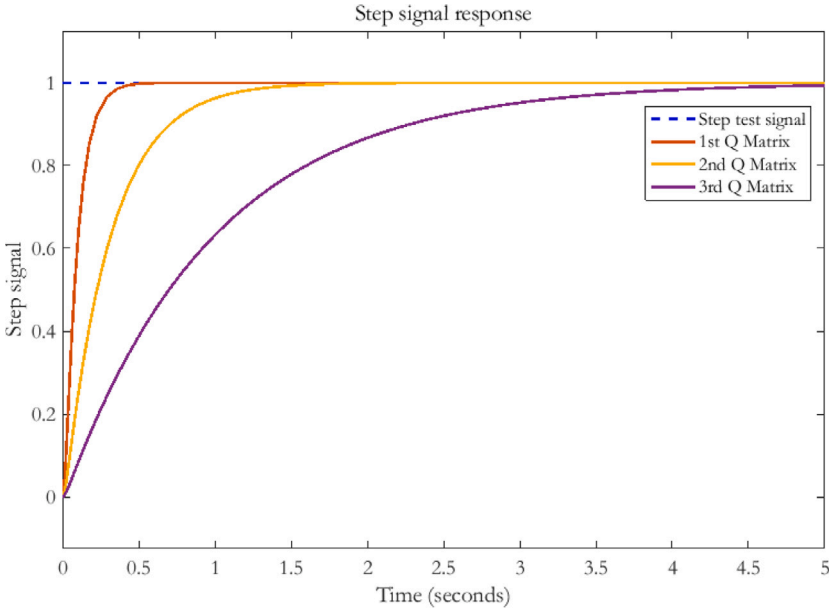

Fig. 8. Comparative response of the step test signal in attitude roll dynamics with gain state feedback using the LQR technique.

Table 5
Comparison of response characteristics after being given a step test signal with gain state feedback using pole placement and LQR.

Characteristic	Gain state feedback with	
	Pole placement	LQR
Rise Time (s)	0.3662	0.1580
Settling Time (s)	0.6551	0.5244
Settling Min	0.9027	0.9121
Settling Max	0.9993	1.0085
Overshoot (%)	0	0

4.3. Noise testing

To see the performance of the $K_{1\phi}$ and $K_{2\phi}$ gain controllers from the results of the LQR method, noise process (disturbance) and noise measurement (output) were added with the response results using the step test signal presented in Fig. 10.

Fig. 10(a) shows the response after only being given process noise, Fig. 10(b) shows the response after only being given output noise and Fig. 10(c) shows the response after being given process noise and output noise. From this testing process it can be seen that the gain state feedback controllers $K_{1\phi} = 10.0000$ and $K_{2\phi} = 1.0051$ cannot overcome the given noise problem, therefore the LQG controller is applied to eliminate noise.

4.4. LQG controller testing for noise

The gain value of state feedback $K_{1\phi}$ and $K_{2\phi}$ using LQG controller can be obtained using MATLAB with the command "$K = lqr((A - LC), B, Q, R)$". But before that, it is necessary first to get the observer gain value in the form of gain L. To get

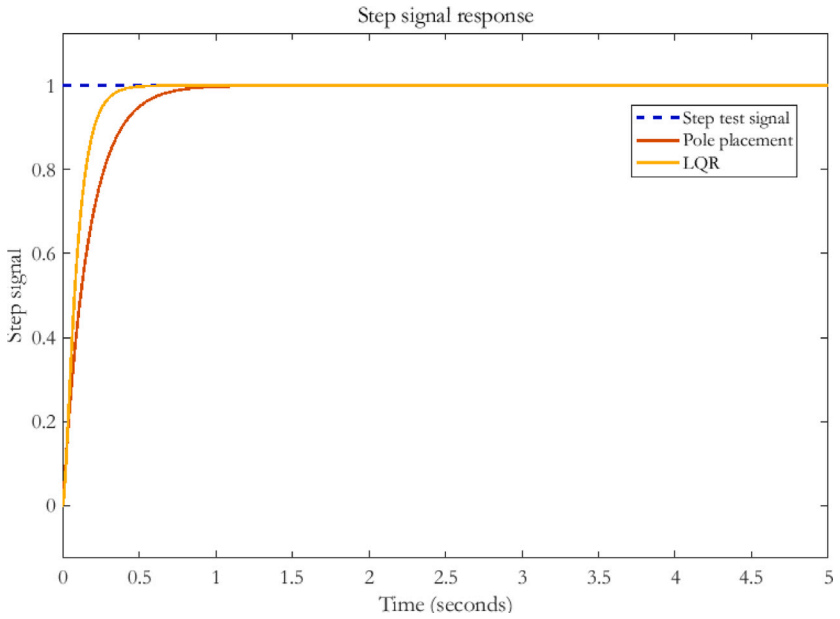

Fig. 9. Comparative response of step test signal with gain state feedback using pole placement and LQR techniques in attitude roll dynamics.

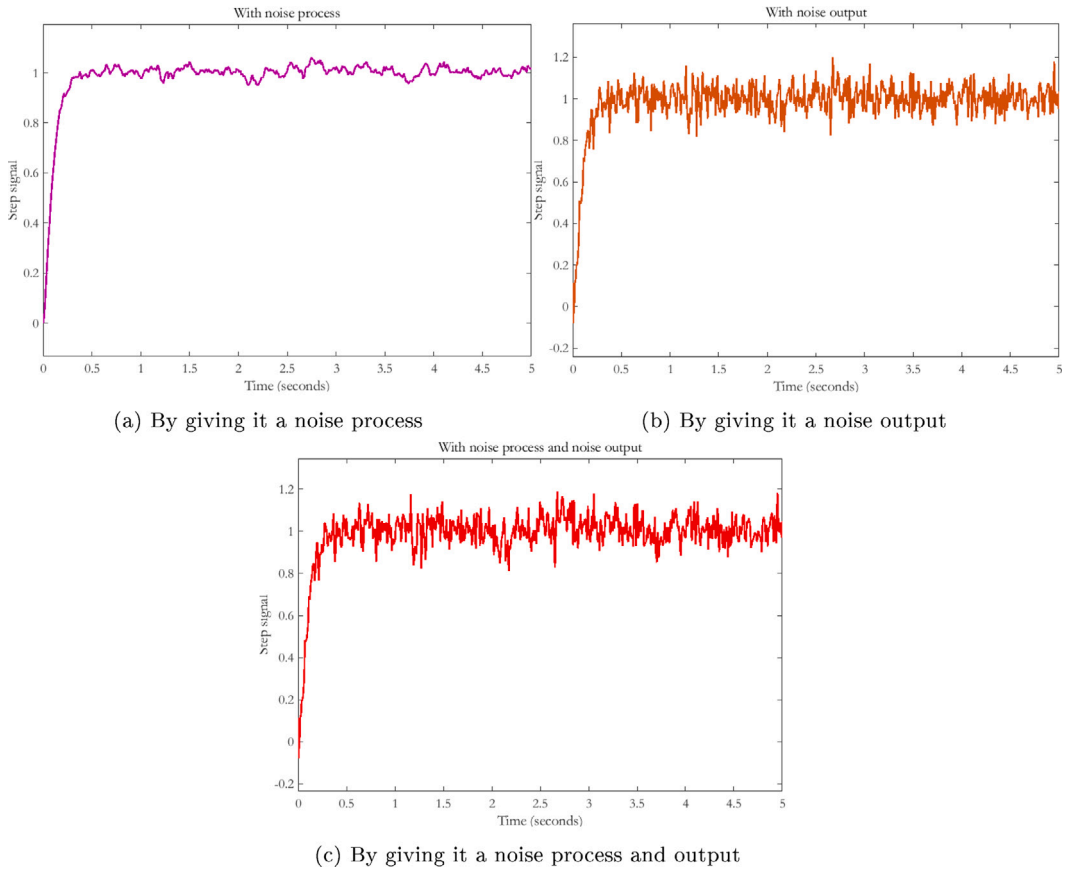

Fig. 10. Step test signal response in attitude roll dynamics with gain state feedback $K_{1\phi} = 10.0000$ and $K_{2\phi} = 1.0051$ after noise.

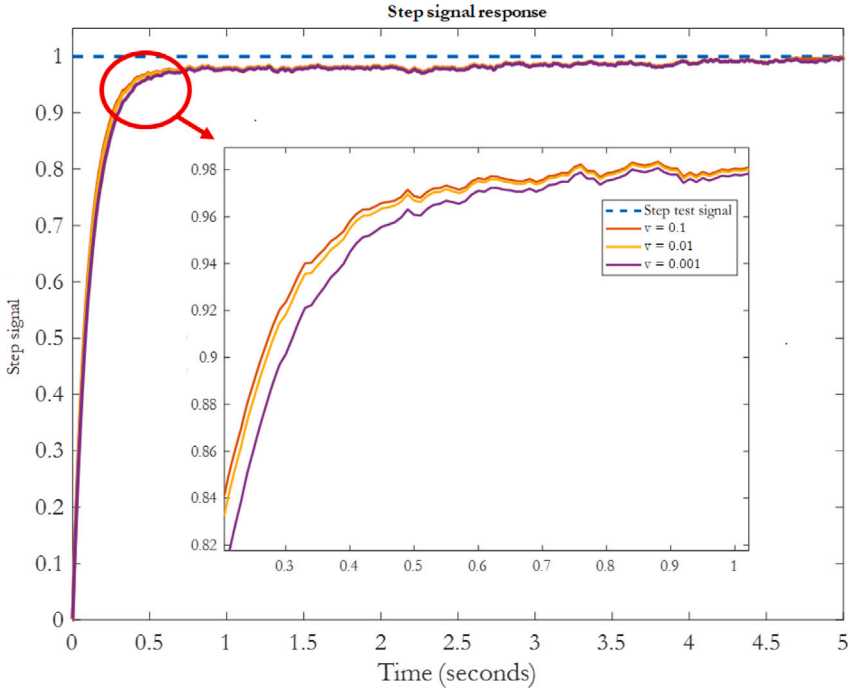

Fig. 11. Comparative response of step test signal on attitude roll dynamics using LQG control after given noise and influence on the value of matrix v.

Table 6
Effect of matrix v on the value of the state feedback gain $K_{1\phi}, K_{2\phi}$.

No	Variation of matrix v value	Gain state feedback value	RMSE value
1	0.1	$K_{1\phi} = 9.5499,\ K_{2\phi} = 1.0049$	0.1606
2	0.01	$K_{1\phi} = 9.1765,\ K_{2\phi} = 1.0047$	0.1635
3	0.001	$K_{1\phi} = 8.4088,\ K_{2\phi} = 1.0043$	0.1832

Table 7
The cubic payload parameter with uncertainty value.

Parameters	Value	Units
Mass (m_d)	= 0.2 + 2.0*random(0-1)	kg
Length (d)	= 0.08 + 0.20*random(0-1)	m
Width (w)	= 0.08 + 0.20*random(0-1)	m
Height (h)	= 0.08 + 0.20*random(0-1)	m

this gain L with the help of MATLAB using the command "$L = lqe(A, w, C, w, v)$". The value of the noise process covariance matrix (w) is set at a value of $0.1 \times eye(2)$ and the noise output covariance matrix (v) is set at the variation of values presented in Table 6 to produce different values of state feedback gain $K_{1\phi}$ and $K_{2\phi}$ with the results of the step test signal response shown in Fig. 11.

4.5. Scenario 3

In the second scenario test, the value of the payload inertia is in a known condition so that the state feedback gain value can be obtained using Eqs. (42) and (43). This condition is not applicable if the cubic value of the payload inertia is unknown, necessitating the use of a controller design to execute the adaptation process. In Table 7, the inertia value of the payload is assigned a random condition value with upper and lower limit conditions during the third scenario test.

This third scenario test utilizes the proposed method that was developed in this research, specifically the LQG adaptive control algorithm outlined in algorithm 1. The proposed adaptive mechanism is an enhancement of LQG control that can track the response of the reference model by incorporating the MRAC approach with the MIT rule. This method utilizes a reference model to establish the response characteristics. Hence, the pole placement technique is a more suitable solution compared to the LQR technique. The reference model employed in this third scenario test is the system characterized by Eq. (57), with pole values of −6 and −325.

The results of the LQG adaptive controller are influenced by the calculation value of ρ obtained in Eq. (58), it can be seen that the value of ρ is influenced by the value of σ, so in the next test, variations of the value of σ are given as in Table 8 so that the results of ρ are presented in Fig. 12 and the response of the step test signal in Fig. 13.

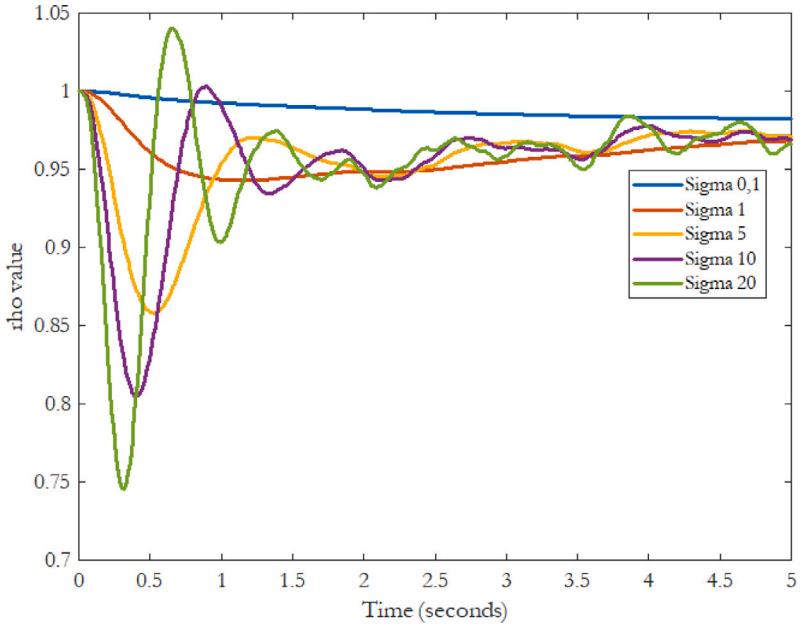

Fig. 12. Signal response of ρ with varying values of σ.

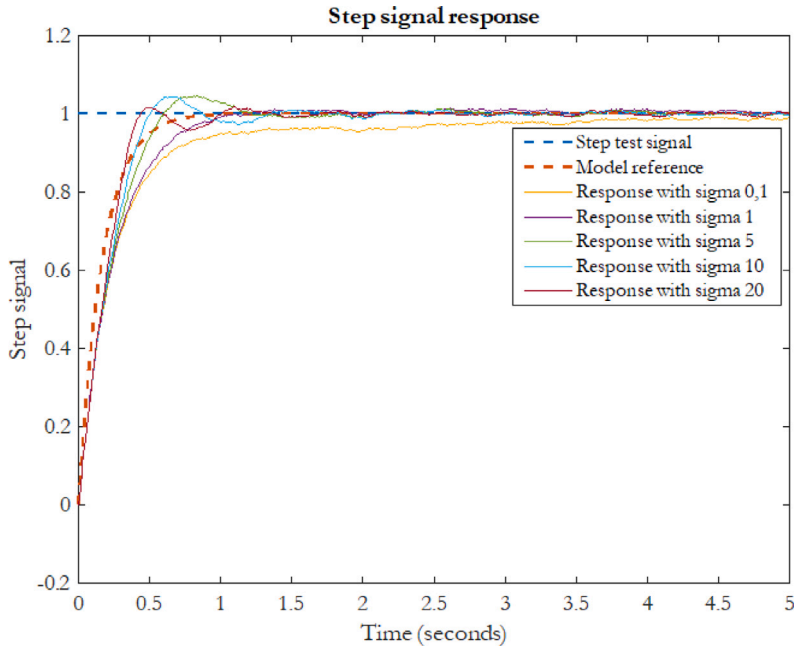

Fig. 13. Comparative response of step test signal on dynamic attitude roll with gain state feedback using adaptive LQG and varying the value of σ.

From Table 8, the best response value for the σ parameter is 20 when observed from the RMSE results. If observed from the overshoot value, $\sigma = 0.1$ produces the lowest value but requires a long settling time (2.5892 s). For $\sigma = 1$ is the ideal value, because the overshoot value is insignificant and has the best settling time of 0.9268 s. To improve performance when using $\sigma = 1$, the ρ gain calculation mechanism designed in Eq. (58) can be developed into Eq. (59). The results of the step test signal response after the development of the ρ gain calculation mechanism are presented in Fig. 14. Table 9 shows that the results of the response characteristics have improved significantly.

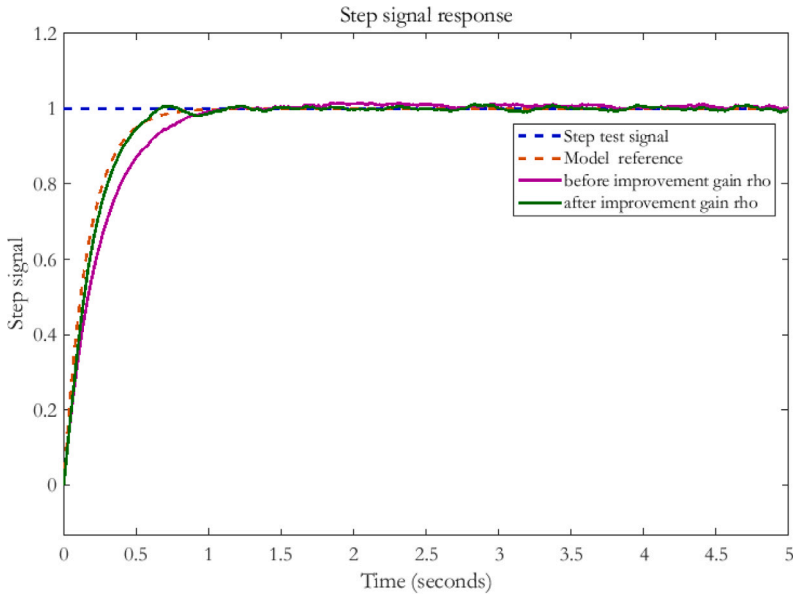

Fig. 14. Comparative response of step test signal on attitude roll dynamics with state feedback gain using adaptive LQG and improvement of gain value ρ.

Table 8
Effect of varying the value of σ.

No	Variations σ value	Rise time (s)	Settling time (s)	Overshoot (%)	Peak	RMSE value
1	0.1	0.5911	2.5892	0.1307	0.9916	0.1763
2	1	0.5430	0.9268	1.4406	1.0148	0.1653
3	5	0.4206	1.1036	4.7296	1.0452	0.1631
4	10	0.3665	1.1814	4.6408	1.0444	0.1576
5	20	0.3169	0.9427	1.7385	1.0185	0.1523

Table 9
Comparison of response characteristics before and after improvement gain value ρ.

Characteristics	Improvement of gain value ρ	
	Before	After
Rise Time (s)	0.5534	0.3831
Settling Time (s)	0.9069	0.5943
Settling Min	0.9027	0.9010
Settling Max	1.0160	1.0105
Overshoot (%)	1.3133	1.2051

5. Conclusion

Simulation of LQG adaptive controller to control attitude roll of bicopter with inertial disturbance in the form of payload has been successfully simulated using MATLAB-Simulink. This paper has successfully designed an adaptive mechanism by developing equations to find the gain ρ in the LQG adaptive controller. There is a parameter σ that affects the result of the gain ρ. This σ parameter acts as a learning rate that produces a response to adapt to the response of the reference model. From the test results obtained when the value of σ is enlarged there is an increased overshoot condition/value but the RMSE value decreases. That means when the RMSE decreases, the response is getting closer to the reference model. To eliminate/reduce the overshoot effect of increasing the value of σ, an improvement is made in finding the gain value of ρ.

The application of LQG adaptive control is still limited to simulation. The designed control system needs to be implemented on hardware. In addition, this research focuses on attitude control. In future research, the attitude control system can be integrated with the position control system to obtain a comprehensive bicopter control system.

Declaration of competing interest

The authors declare that they have no known competing financial interests or personal relationships that could have appeared to influence the work reported in this paper.

Data availability

Data will be made available on request.

References

[1] Albayrak ÖB, Ersan Y, Bağbaşı AS, Başaranoğlu AT, Arıkan KB. Design of a robotic bicopter. In: 2019 7th international conference on control, mechatronics and automation. IEEE; 2019, p. 98–103.
[2] Zhang Q, Liu Z, Zhao J, Zhang S. Modeling and attitude control of bi-copter. In: 2016 IEEE international conference on aircraft utility systems. IEEE; 2016, p. 172–6.
[3] Hrečko L, Slačka J, Halás M. Bicopter stabilization based on IMU sensors. In: 2015 20th international conference on process control. IEEE; 2015, p. 192–7.
[4] Visioli A. Practical PID control. Springer Science & Business Media; 2006.
[5] Li Y, Qin Y, Xu W, Zhang F. Modeling, identification, and control of non-minimum phase dynamics of bi-copter uavs. In: 2020 IEEE/aSME international conference on advanced intelligent mechatronics. IEEE; 2020, p. 1249–55.
[6] Büchi R. State space control, LQR and Observer: step by step introduction, with Matlab examples. Books on Demand; 2010.
[7] Hendricks E, Jannerup O, Sørensen PH. Linear systems control: deterministic and stochastic methods. Springer; 2008.
[8] Hong J-Y, Chiu P-J, Pong C-D, Lan C-Y. Attitude and altitude control design and implementation of quadrotor using NI myrio. Electronics 2023;12(7):1526.
[9] Qin Y, Xu W, Lee A, Zhang F. Gemini: A compact yet efficient bi-copter uav for indoor applications. IEEE Robot Autom Lett 2020;5(2):3213–20.
[10] Qin Y, Chen N, Cai Y, Xu W, Zhang F. Gemini II: Design, modeling, and control of a compact yet efficient servoless bi-copter. IEEE/ASME Trans Mechatronics 2022.
[11] He X, Wang Y. Design and trajectory tracking control of a new bi-copter UAV. IEEE Robot Autom Lett 2022;7(4):9191–8.
[12] Hu A, Zhao X, Xu D. Modeling and hovering control of 5-DoF tilt-birotor robot. In: 2020 16th international conference on control, automation, robotics and vision. IEEE; 2020, p. 572–7.
[13] Khalil HK. Lyapunov stability. Control Syst Robot Autom 2009;12:115.
[14] Unser M. A note on BIBO stability. IEEE Trans Signal Process 2020;68:5904–13.
[15] Selvam A, Sabarinathan S, Pinelas S. The aboodh transform techniques to Ulam type stability of linear delay differential equation. Int J Appl Comput Math 2023;9(5):115.
[16] Pinelas S, Selvam A, Sabarinathan S. Ulam–Hyers stability of linear differential equation with general transform. Symmetry 2023;15(11):2023.
[17] Abedini A, Bataleblu AA, Roshanian J. Robust backstepping control of position and attitude for a bi-copter drone. In: 2021 9th RSI international conference on robotics and mechatronics. IEEE; 2021, p. 425–32.
[18] Astrom KJ. Adaptive control around 1960. IEEE Control Syst Mag 1996;16(3):44–9.